DERIVATION OF CONSTITUTIVE LAW FOR UHPFRC USING DIC SYSTEM

Tamás Mészöly (1), Norbert Randl (1)

(1) Carinthia University of Applied Sciences, Spittal an der Drau, Austria

Abstract

An accurate constitutive law for ultra-high performance fibre-reinforced concrete (UHPFRC) is necessary to model or design structures using this material. The present study is based on large sets of experimental tests (compression tests, modulus of elasticity tests, splitting tensile tests, uniaxial tensile tests and flexural tests) to derive full constitutive laws of different UHPFRC recipes with special interest on the tensile behaviour and the effect of the fibres. By using a Digital Image Correlation (DIC) system it is possible to directly derive the surface deformations in any point or the crack opening of every single crack. In the frame of this study a number of flexural tests provided with traditional and with DIC measurement system were performed. An in-depth comparison of all measurement results was performed and the tensile behaviour of the used UHPFRC was analysed. The applicability of the DIC recordings to the evaluation procedures defined in existing guidelines which rely on traditional measurement methods is investigated and presented.

Résumé

Une loi de comportement précise du béton fibré à ultra-hautes performances (BFUP) est nécessaire pour calculer ou concevoir des structures utilisant ce matériau. L’étude présentée est basée sur un large ensemble de tests expérimentaux (essais de compression, de module d’élasticité, résistances en traction par fendage, essais de traction uni-axiale et essais de flexion) pour en déduire les lois de comportements des différentes formules de BFUP avec un intérêt particulier sur le comportement en traction et sur l’effet des fibres. Par l’utilisation d’un système automatisé de corrélation d’images il est possible de calculer directement les déformations de surface en tout point ou l’ouverture de chaque fissure. Dans le cadre de cette étude un certain nombre d’essais de flexion ont été effectués avec une extensométrie traditionnelle et par analyse d’images. Une comparaison approfondie des résultats des mesures a été effectuée et le comportement en traction du BFUP utilisé a été analysé. L’applicabilité des enregistrements de corrélation d’images aux procédures d’évaluation définie dans les recommandations existantes qui repose sur des méthodes de mesure traditionnelles est étudiée et présentée.

1. INTRODUCTION

Knowledge of the constitutive law of the used concrete is generally necessary to model or design concrete structures. While ordinary RC design usually does not take into account the tensile resistance of a concrete cross-section, this is much more important when using high performance fibre-reinforced concrete. In the last twenty years intensive research has been conducted in this field and meanwhile some well-known guidelines are available (e.g. [1, 2, 3]). The approaches differ from each other with respect to the required specimen production, geometry, testing method, measurement setup and evaluation of the acquired data, thus resulting in deviating constitutive laws.

Splitting tensile test can provide useful information about the tensile behaviour, but if the complete relation between the tensile stress and the tensile strain is needed, direct (uniaxial) tensile tests or flexural bending tests are the most commonly conducted tests. Because of practical difficulties with the direct tensile tests, latest guidelines recommend to use the indirect derivation via flexural tensile tests [1, 2].

The AFGC Guideline [2] recommends a minimum number of six four-point bending tests on un-notched prismatic specimens to determine the flexural strength and the end of the elastic part. In addition a minimum number of six three-point bending tests on notched prismatic specimens are also required to determine the post-cracking behaviour and the stress vs. crack opening and the stress vs. strain relations.

Other guidelines such as the RILEM recommendation [4], JCI recommendation [5] or the German Guideline for fibre-reinforced concrete [6] require different setups and testing procedures. According to [6, 7] four-point bending tests on un-notched specimens are recommended to derive the constitutive law in tension. In this study three series of tests in four-point bending test setup on un-notched specimens were tested and evaluated.

A correct recording of all required measurement data is the precondition for an accurate derivation of the constitutive law. Traditional measurement methods (using for instance strain gauges, displacement transducers or strain transducers) often lead to misinterpretations because of multiple cracking, inclusion of elastic deformations in the measurement or inaccurate identification of the cracking force. A Digital Image Correlation (DIC) measurement system is an effective tool to measure and monitor structural deformations with high accuracy, and its usage is more and more common in research and engineering practice [8]. Therefore in this context both traditional and DIC measurement are used to provide comparative data sets.

2. TEST SERIES

2.1 Material properties

Three series of tests were performed: Series “F1” with 1.35 Vol.-% fibres, series “F2” with 1.75 Vol.-% fibres and series “F3” with 2.00 Vol.-% fibres. The UHPC concrete matrix was the same for the three series, using a maximum grain size of 0.8 mm. The water to cement ratio was 0.25, the water to binder ratio 0.22. The mean value of the compressive strength measured on cubes with a side length of 100 mm was around 170 MPa and modulus of elasticity around 51 GPa.

2.2 Test setup

Tests were performed in a four-point bending test setup with a span of 600 mm according to the German guidelines [6, 7]. Test setup and dimensions of the test specimens are shown in Figure 1. A number of six un-noched specimens were tested per series, and the following measurements were recorded:

- applied force
- way of the cylinder
- deflection using linear variable displacement transformers (LVDT)
- crack opening using strain transducers (DD1 from HBM)
- strain of the top of the (compressed) concrete using strain gauges
- displacement of the surface points using a Digital Image Correlation (DIC) measurement system.

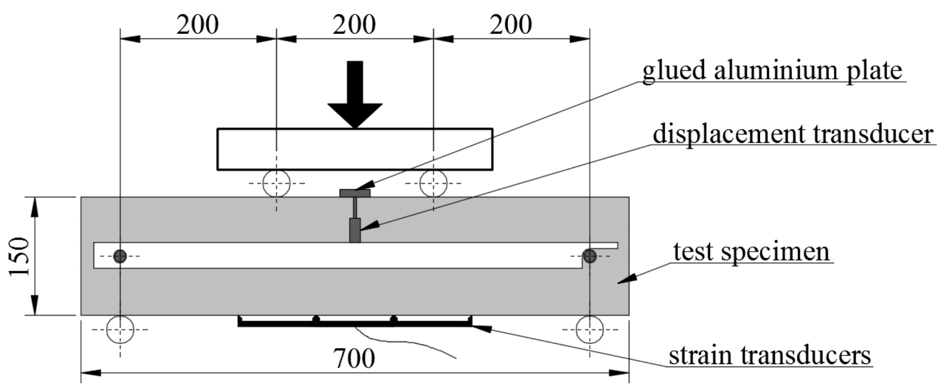

Figure 1: Test setup and dimensions of the specimens

Figure 2 shows some pictures of the tests. The left picture shows the DIC measurement system, the middle picture the test setup and the screen with the live values of the sensors, the right-top picture the strain gauge on the top of the beam and right-bottom picture the strain transducers (3 sensors with a base length of 100 mm).

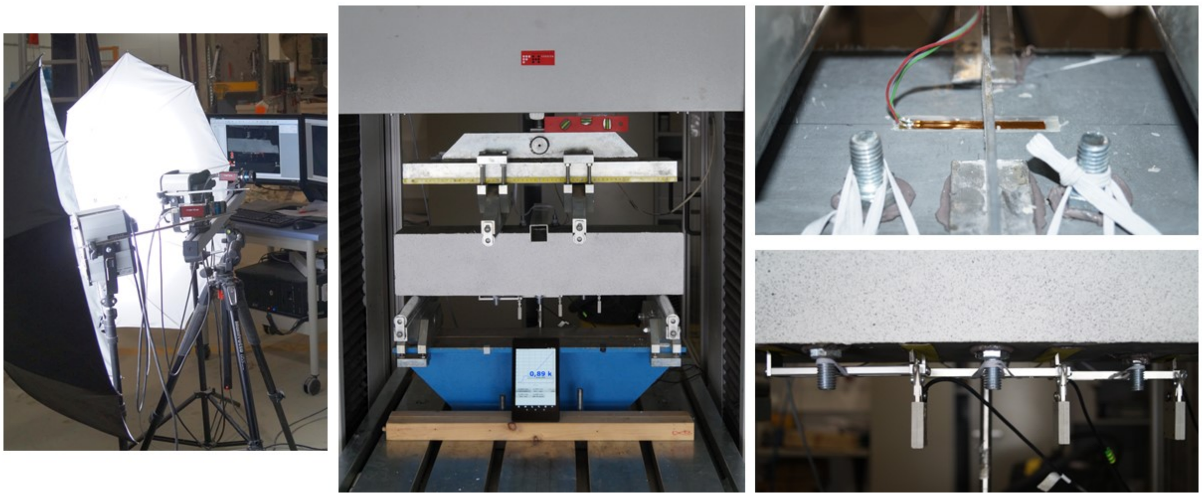

Figure 2: Test setup and measurements of the flexural tests

3. TEST RESULTS

In order to derive the full constitutive law in tension, the force vs. deflection curves and the related crack propagation have to be taken into account. In the following sections, the results from both traditional and DIC measurements are displayed and compared to each other.

3.1 Flexural stress vs. deflection curves

The basic results were the load vs. deflection curves, since these values were measured directly during the test. The applied load was measured in the testing equipment by a built-in load cell. The deflection was measured at the middle of the specimens by an LVDT.

From the applied load the flexural tensile stress was calculated at the bottom of the beam. The flexural tensile stress vs. deflection curves together with the calculated mean curves for each series are shown in Figure 3. This is a commonly used way to compare the efficiency of the different fibre constellations and the tensile behaviour of the different concrete mixtures. The scatter of these results is usually high because of the different fibre orientation and fibre distribution of the specimens. The mean values of the flexural tensile strength were 14.1 MPa for series *F1*, 16.8 MPa for *F2* and 22.1 MPa for *F3*. The coefficients of variation were 21 %, 14 % and 11% for *F1*, *F2* and *F3*, respectively. Series *F3* worked the best according to the flexural strength values and their scatter. The mean value of the deflection at maximum force (or at maximum flexural tensile stress) was between 1.1 mm and 1.2 mm for series *F1* and between 1.3 mm and 1.4 mm for *F2* and *F3*.

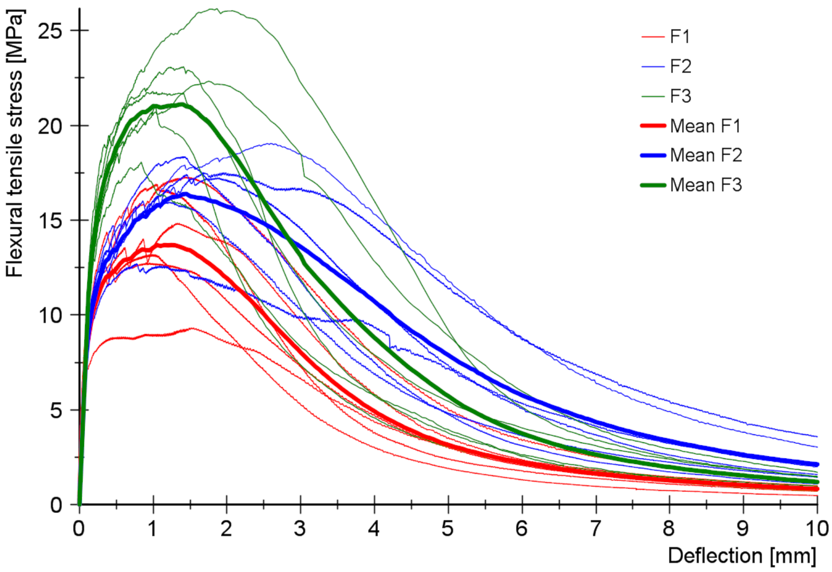

Figure 3: Flexural stress vs. deflection curves

3.2 Crack pattern

Digital Image Correlation (DIC) technique is a useful tool to measure and monitor the structural deformations. It is possible to directly measure the surface deformations accurately (three dimensional absolute and relative movements, or strain values in any point in any direction) or the crack opening values of every single crack. It provides different types of measurements than displacement transducers, strain gauges and strain transducers, and both approaches can effectively complete each other. Deriving the tensile behaviour of a fibre-reinforced concrete is possible with both measurement solutions, and in this research project both approaches were used simultaneously.

One of the main results from the DIC measurements is the crack pattern of the test specimens at any stage of the tests. The number of cracks is one of the indicators about the fibre efficiency and the stress distribution, and the distribution of the cracks is a second indicator. Just one crack or only a few numbers of larger cracks in a specimen means that the fibres are not effective enough, and this is usually accompanied by low results and rigid failure at the flexural bending tests. Larger numbers of smaller cracks with similar distance mean that the fibres are effective and the fibre-reinforced concrete mixture is closer to a homogeneous material with a considerable tensile strength. The first type of concrete is usually classified as strain-softening concrete and the second type is usually classified as (low or high) strain-hardening concrete.

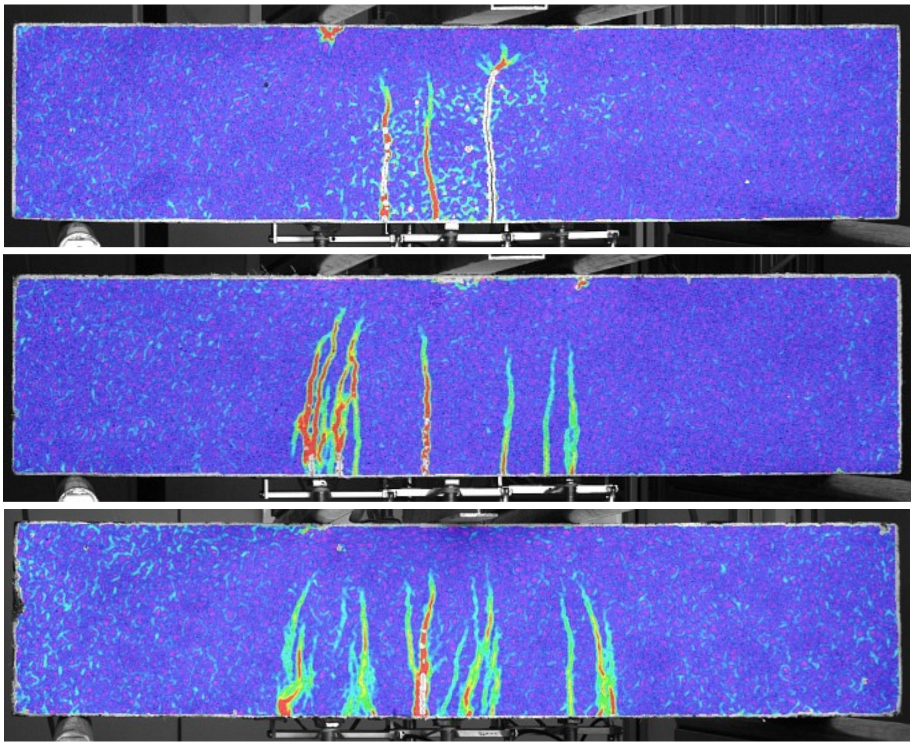

Figure 4: Typical crack pattern of each series

Figure 4 shows the typical crack pattern of each series *F1* to *F3* close to the reached maximum load. While in case of non-reinforced, rigid materials cracks have sharp, smooth edges and are usually separated from each other, in case of fibre-reinforced concrete counting the number of cracks is not always easy or clear. Edges of the cracks are in this case usually rough; many cracks occur in groups, most of them have several branches, many of them cross each other with common and separated sections, and the crack pattern change continuously during the test. In this study cracks were counted and measured on the bottom edge of the bended beam. Where it was possible, they were measured separately, but in case they appeared in groups or very close to each other, they were counted as one crack. Using this process, the mean number of cracks was around 4 for series *F1* and close to 9 for *F2* and *F3*.

3.3 Crack opening

Elongation of the bottom side of the beam was measured and the progress of the crack opening process in parallel with the DIC system (using virtual extensometers) and with strain transducers (using DD1 sensors from HBM) was monitored. In case of the DIC system every single crack on the whole length of the beams (700 mm) was identified, and crack opening measurements were performed on the bottom edge of the side of the beams (see also description in section 3.2). The base length of the applied virtual extensometers was between 5 mm and 10 mm. In case of the strain transducers, measurements were performed on the bottom surface in the middle of the beam on a length of 300 mm. This length was covered by three stain gauges with a base length of 100 mm each.

The observed load bearing behaviour can be subdivided into three main stages: The first one is the elastic part until the concrete matrix reaches its tensile strength and the first bending crack appears. The second stage is the micro-cracking with formation of several smaller cracks with similar size. The third phase starts when one crack becomes the decisive one (in consequence representing the failure surface between the two beam parts after breakage) and all the other cracks stop increasing or rather tend to close at least partly. In this last phase the beam behaves more and more like two rigid parts interconnected via a plastic hinge.

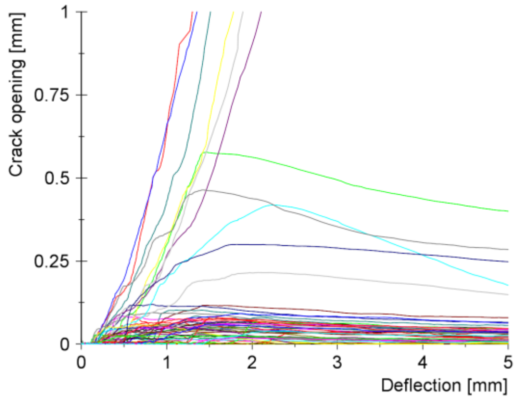

Figure 5: Crack opening vs. deflection curves

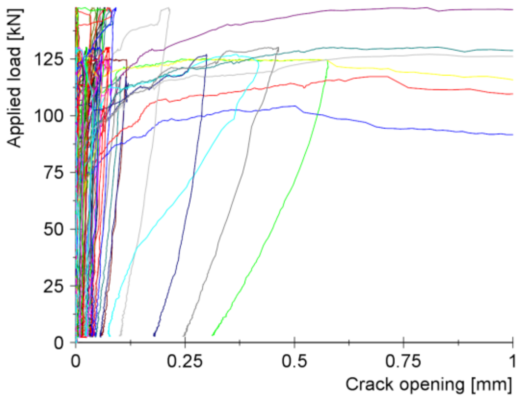

Figure 6: Flexural stress vs. crack opening

Figure 5 displays the crack opening vs. deflection curves and Figure 6 the flexural tensile stress vs. crack opening curves for series *F3* (results derived from the DIC system). From the curves it can be seen that most of the cracks stayed smaller than 0.1-0.12 mm, just very few cracks (typically only one crack per beam) reached a maximum crack opening between 0.12 mm and 0.6 mm, and one crack from each test opened widely and formed later the point of failure. The mean value of the crack opening of the largest crack at the maximum applied load was 0.92 mm for series *F1*, 0.89 mm for *F2* and 0.70 mm for *F3* with the coefficient of variation of 45 %, 25 % and 19 %, respectively. These crack openings are comparable to results from other researchers, who measured values between 0.4 mm and 2.0 mm [3].

Figure 7 shows the typical recorded crack opening vs. time curves from both types of sensors. From the results it can be concluded that both types of measurement (with an accuracy of 1 µm to 2 µm) are sensitive enough to recognize the cracking load (load level where the first crack appears) and follow the cracking process already in the crack formation phase (below 10-20 µm [9]). The AFGC Guideline [2] defines the stress corresponding to the beginning of cracking (matrix strength or elastic strength) as the point of the loss of linearity, but determination of this point is usually provide an around ±10% accuracy. Usage of the crack opening curves allows the identification of the moment where the first crack appears and the cracking process starts. In the present study, the according values were 5.6 MPa for series *F1*, 6.6 MPa for *F2* and 11.9 MPa for *F3* with the coefficient of variation of 14% (*F1* and *F2*) and 8% for *F3*. These strength values must be corrected using adequate formulae [1, 2] to take the scale effect into account and thus receive the (direct or uniaxial) tensile strength of the matrix. The equation according to AFGC [2] gives a factor of 0.73 in this case and the corrected tensile strength values are 4.1 MPa, 4.8 MPa, and 8.7 MPa for the three series.

Figure 7 shows that after formation of the first crack many other small cracks occurred at different load levels. The multi-cracking mechanism of UHPFRC was described by other researcher already [2, 10, 11] and depends on the fibre content. The strain transducers usually measure the sum of more (2-6) cracks on their measurement base length (100 mm). For comparison the crack opening curves from the DIC system were added together and compared with the values from the strain transducers (see in Figure 8 for one beam).

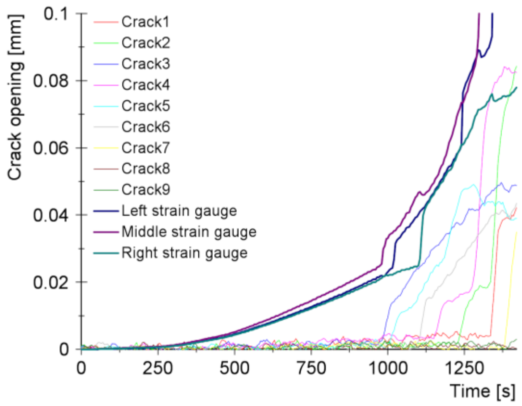

Figure 7: Strain transducers vs. DIC system

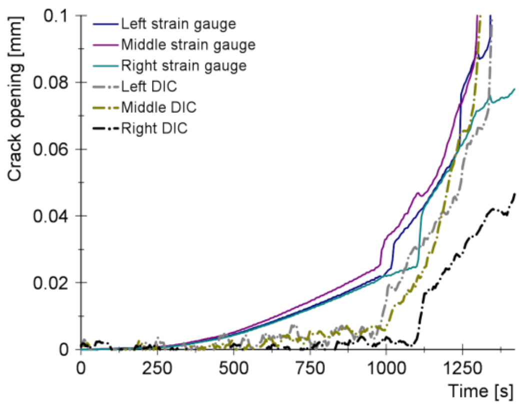

Figure 8: Strain transducers vs. DIC system

While values from the strain transducers are more accurate and show less measurement noise, the range of measurement is limited to ±2.5 mm and the sensors measure along their base length more cracks together with the elastic elongation of the uncracked part of the concrete. In case of the image correlation the measurement range is not limited. The system can measure the cracks separately and the effect of the elastic elongation in the measurement is about twenty times smaller (in case of the combined curves this ratio is around five). Figure 8 shows that the corresponding curve-pairs are similar, but because of the mistakenly measured elastic deformation they are shifted from each other. Figure 9 shows the crack opening vs. time curves (until a crack opening of 2.0 mm) and Figure 10 shows the crack opening vs deflection curves for the same beam (cf. Figure 5) after removal of the initial elastic deformation. The curve-pairs are very close to each other and show that both measurement systems provide comparable and trustable results. The small difference may result from some micro-cracks not taken into account with the DIC system. Moreover some single cracks are outside the 300 mm measured range and therefore not recorded by the tensile transducers; however, the difference can also be attributed to differences between the two sides of the beam (DIC system recorded the front surface while DD1 sensors measured on the bottom side). The investigation described above was performed with all beams with very similar curves, results and conclusions.

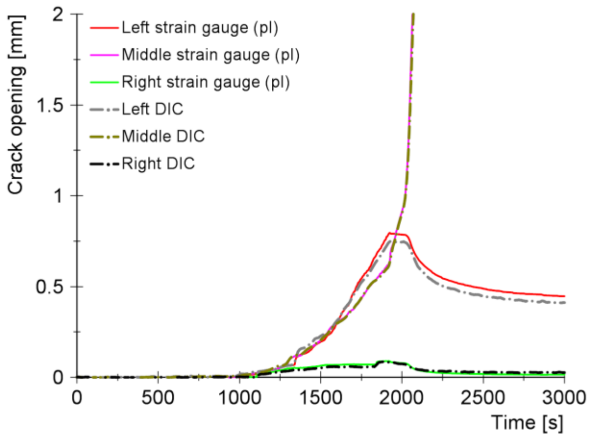

Figure 9: Without elastic deformation

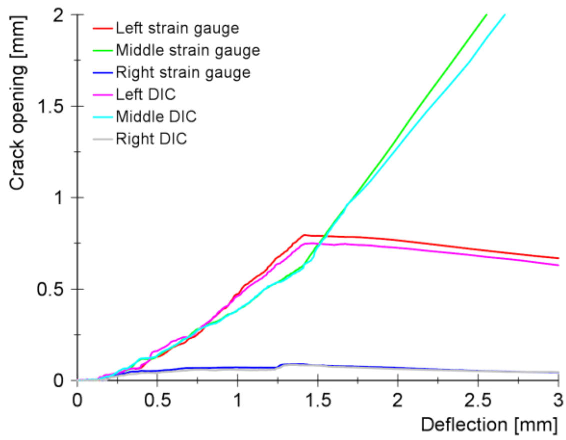

Figure 10: Without elastic deformation

4. TENSILE STRESS CURVES

With the applied load vs. crack opening curves it is possible to indirectly derive the tensile stress vs. crack opening curves using the method named inverse analysis or back analysis [2, 12]. For this calculation the crack opening curve of the decisive crack (see explanation in section 3.3) was used for each beam. Figure 11 shows exemplarily the derived tensile stress vs. crack opening curves for series *F3*.

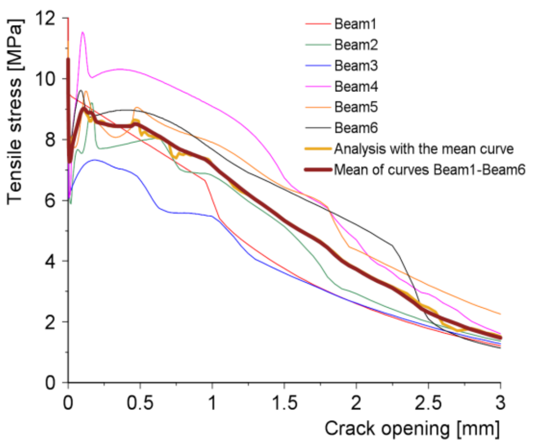

Figure 11: Tensile stress vs. crack opening

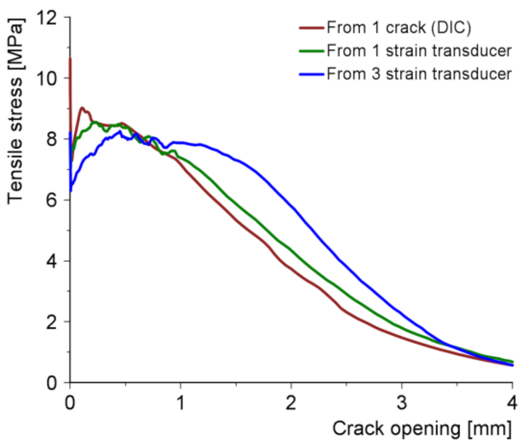

Figure 12: Effect of the base length

Figure 11 also shows that there is no significant difference in considering each single test curve and executing back analysis or derive first the mean curve from all test in one series and then perform inverse analysis.

There is a theoretical problem with this approach: The theory of the inverse analysis is based on the formation of one crack, but in case of fibre-reinforced concrete and four-point bending test setup, there are always a number of cracks [2, 11]. With three-point bending tests on notched specimens this problem can be avoided, but this is not always reasonable or, with respect to certain guidelines, legally possible. Therefore it is important to clarify the effect of multi-cracking on the evaluation procedure and the test results.

First, usually not the first crack (which determines the end of the elastic part and the matrix strength) will be the decisive crack later on. Therefore the tensile stress curves, derived using the decisive crack, do not coincide with the tensile strength derived from the first crack.

Secondly, section 3.3 showed that the decisive crack is dominant in the post-peak part of the tests, but in the second, micro-cracking stage other cracks are in the same magnitude, and multi-cracking can affect significantly the derived tensile stress curves. To investigate this, inverse analysis was executed on the applied force vs. crack opening curves from the decisive crack (measured by the DIC system) and from the summed up crack opening values measured by the strain transducer (base length of 100 mm) at the position of the decisive crack. Additionally, inverse analysis was executed on a curve derived by adding the crack opening values of the three strain transducers together (base length of 300 mm). This gives nearly the same result compared to summarizing all crack opening curves from the DIC system. Figure 12 depicts the results from these three types of calculation for series *F3*. The difference between the calculation with the crack opening from the decisive crack and from the elongation measured with one strain transducer is rather small. However, when calculating with the crack openings summed up over the 300 mm measurement length, the difference becomes more significant. Although the difference was usually smaller, already a small change of the tensile stress curve can cause significant difference in the bending behaviour of structural elements without ordinary reinforcing bars or the structural behaviour in shear [13].

Figure 13 and Figure 14 show a comparison of the results from different series. Figure 13 shows the tensile stress vs. crack opening curves from series *F2* and *F3*, and Figure 14 shows the tensile stress vs. strain relations for the same series. In order to calculate the tensile strain from the crack opening values, the approach of the AFGC Guidelines [2] was used.

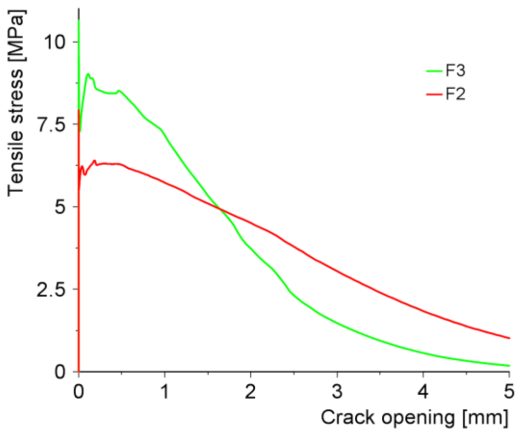

Figure 13: Tensile stress vs. crack opening

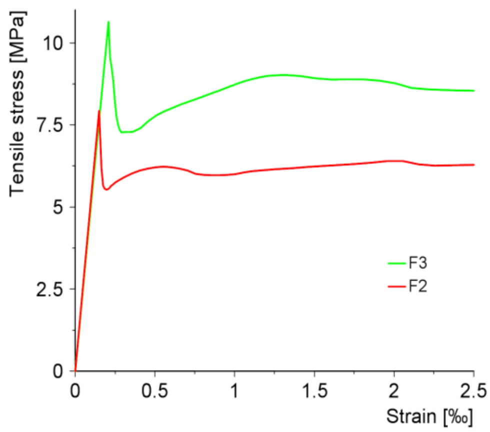

Figure 14: Tensile stress vs. strain relation

5. CONCLUSIONS

Three series of four-point bending tests on prismatic and un-notched UHPFRC specimens were performed to determine the behaviour in tension in order to verify the applicability of an alternative measurement system.

The traditional measurement system (displacement transducers, strain gauges and strain transducers) and a Digital Image Correlation system were used in parallel and the results from the two types of measurement systems were compared. The DIC system provides accurate and trustable results for every single crack. The system was able to monitor the crack opening, crack development and the changing crack pattern from the early crack formation until failure. The derived crack opening curves were useful for the sensitive inverse analysis and to derive the tensile side of the constitutive law based on the virtual measurements. With this measurement technique it is also possible to separate the elastic and plastic parts of the deformation, which are measured together with the commonly used sensors (displacement and strain transducers).

Evaluation of the tests showed that series *F3* provided the best results for the compression strength, tensile properties and workability, compared to series *F1* and *F2*.

Four-point bending tests on un-notched specimens together with the DIC system can deliver detailed information about the multi-cracking behaviour and the failure mechanism and thus contribute to improve the evaluation approach based on the theoretical background.

ACKNOWLEDGEMENTS

The presented study is part of a research program carried out in cooperation with Graz University of Technology and the industrial partners Voestalpine Special Wire GmbH and Kirchdorfer Industries GmbH. The funding of the project by the Austrian Research Promotion Agency (FFG) and the above mentioned industrial partners is greatly acknowledged.

REFERENCES

[1] Fédération internationale du béton, 'fib Model Code for Concrete Structures 2010' (Wilhelm Ernst & Sohn, Lausanne, 2012).

[2] Association Française de Génie Civil, 'Ultra High Performance Fibre-Reinforced Concretes – Recommendations', Revised ed., (Association Française de Génie Civil (AFGC), June 2013).

[3] Schmidt, M. et al., 'Sachstandsbericht Ultrahochfester Beton', DAfStb **561** (Beuth, 2008).

[4] RILEM TC 162-TDF, 'Test and design methods for steel fibre reinforced concrete: bending test', *Materials and Structures* **35**(253) (2002) 579–582.

[5] Japan Concrete Institute, 'Method of test for load-displacement curve of fiber reinforced concrete by use of notched beam (JCI-S-002-2003)', (2003).

[6] Deutscher Ausschuss für Stahlbeton, 'DAfStb-Richtlinie Stahlfaserbeton – Teil 2' (2012).

[7] Deutschen Beton- und Bautechnik-Verein, 'DBV-Merkblatt Stahlfaserbeton' (2001).

[8] Skarżyński, Ł., Kozicki, J., Tejchman, J., 'Application of DIC Technique to Concrete—Study on Objectivity of Measured Surface Displacements', *Exp. Mechanics* **53**(9) (2013) 1545–1559.

[9] Hillerborg, A., Modéer, M., Petersson P.E., 'Analysis of crack formation and crack growth in concrete by means of fracture mechanics and finite elements', *Cement and Concrete Research* **6**(6) 773-782, (Pergamon Press, United States, 1976).

[10] Jungwirth, J., 'Zum Tragverhalten von zugbeanspruchten Bauteilen aus Ultra-Hochleistungs-Faserbeton', (Doctoral thesis, École Polytechnique Fédérale de Lausanne, 2006).

[11] López, J.Á., Serna, P., Navarro-Gregori, J., Coll, H., 'A simplified five-point inverse analysis method to determine the tensile properties of UHPFRC from unnotched four-point bending tests', *Composites Part B: Engineering* **91** (Elsevier, 2016) 189–204.

[12] Chanvillard, G., 'Caractérisation des performances d'un béton renforcé de fibres á partir d'un essai de flexion - Partie 1: De la subjectivité des indices de ténacité', *Materials and Structures* **32**(6) (Springer, 1999) 418–426.

[13] Randl, N., Mészöly, T., Harsányi, P., 'Load bearing behaviour of slender UHPC beam members in shear', Proceedings of HiPerMat 2016, Kassel (Kassel University Press, Kassel, 2016) 59–60.